Journal of Transport System Engineering 6:1 (2019) 17–32

TRIBOLOGICAL ANALYSIS ON THE EFFECT OF HEAT TRANSFER TOWARDS ENGINE IN-CYLINDER FRICTION

J.Y. Fong[a] and W.W.F. Chong[b]

[a] School of Mechanical Engineering
Faculty of Engineering,
Universiti Teknologi Malaysia,
81310 Skudai, Johor, Malaysia

[b] Department of Aeronautics, Automotive & Ocean,
School of Mechanical Engineering
Faculty of Engineering,
Universiti Teknologi Malaysia,
81310 Skudai, Johor, Malaysia

Article history
Received
27 November 2019
Received in revised form
23 December 2019
Accepted
18 December 2019
Published Online
29 December 2019

*Corresponding author
william@utm.my

GRAPHICAL ABSTRACT

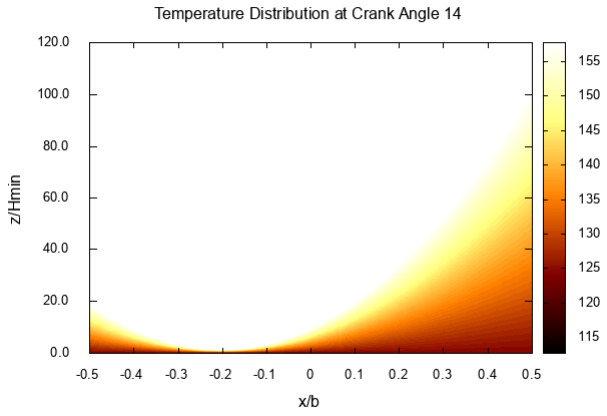

KEYWORDS

Piston ring; tribology; heat transfer; 1-D Reynolds equation; engine in-cylinder friction

ABSTRACT

The aim of this study is to determine the effect of heat transfer towards engine in-cylinder frictional losses, generated by the piston ring pack sliding along the engine cylinder liner. A mathematical model is derived from the 1D Reynolds equation, using Reynolds' boundary condition, to determine the contact pressure distribution along the ring-liner conjunction. Meanwhile, the lubricant temperature profile is solved using the 1D energy equation, considering heat conduction and viscous heating effect. The mathematical models are implemented in C-program. The minimum film thickness and the total friction force from the current model are showing good correlation with literature data. The results showed that heat conduction mechanism predominates the viscous heating effect in the ring-liner conjunction. Meanwhile, the boundary friction predominates the contribution of viscous friction, especially along the vicinity of dead centres. However, the boundary friction is not affected by the changes in lubricant viscosity. Hence, from an overall engine operation point of view, the effect of heat transfer towards the total friction force generated by the ring pack could be considered trivial.

1.0 INTRODUCTION

Despite the well-established technological development in the automotive industry, a considerable amount of energy is still being used to overcome friction. Based on the statistical studies by Holmberg, Andersson and Erdemir (2012), the piston assembly in the engine contributes to the highest frictional losses, which is about 45% out of the 11.5% total of fuel energy used to overcome friction in engine. Hence, a reduction in frictional losses in the piston ring pack is expected to give a significant impact in reducing wastage of fuel, which in turn could lead to an increase in the fuel economy of a vehicle.

The role of the piston ring pack in an internal combustion engine is to form a dynamic seal between the combustion chamber and the crankcase, while the lubricant serves as a medium to separate the ring pack and the cylinder liner. If the sealing performance is poor, there will be a loss in pressure in the combustion chamber during the compression, explosion and expansion stages of the engine cycle. Thus, this could lead to a reduction in power output and efficiency (Rahmani et al., 2017).

In a typical piston ring pack for internal combustion engine, there are three types of piston rings, namely top compression ring, second compression ring and oil control ring. Since all the rings have different types of profile, this will affect the lubricant entrainment into ring-liner contact. Therefore, it is very important to understand the relationship between different ring profiles and the tribological behaviour. This is because they are crucial in lowering the frictional losses in the piston ring-liner conjunction.

Heat transfer in the lubricant has an impact towards the tribological properties along the ring-liner conjunction. Viscosity of the lubricant drops concomitantly with the increase in the fluid film temperature. As a result, the film thickness as well as the load-carrying capacity could be reduced significantly as a result of thermal effects (Hamrock et al., 2004). Hence, the present study intends to determine the extent of heat transfer effects toward the frictional properties of the ring packs with the cylinder liner.

2.0 MATHEMATICAL MODELS

2.1 1-D REYNOLDS' EQUATION

The Reynolds equation is then used to solve for the pressure distribution in the lubrication film, which in turn be used to determine the minimum lubrication film thickness of the lubrication film. The piston ring-liner sliding contact is approximated as an infinitely long bearing without side leakage in the present analysis. Several assumptions are made and they are listed below:

1) Laminar flow due to low Reynolds numbers
2) Newtonian fluid (No slip at boundaries)
3) Constant pressure across the film
4) Negligible inertia and surface tension forces
5) Incompressible flow

Hence, the 1-D Reynolds equation used for solving the contact pressure in the piston ring-liner conjunction can be given as:

$$\frac{\partial}{\partial x}\left(\frac{h^3}{\eta}\frac{\partial P}{\partial x}\right) = 6\left\{\frac{\partial}{\partial x}(U_1 + U_2)h\right\} \quad (1)$$

where h is the lubricant film thickness, P is the contact pressure, η is the lubricant dynamic viscosity, U is the lubricant entrainment velocity and x is the ring width.

2.2 LUBRICANT FILM THICKNESS

A general film thickness equation was used to incorporate with different piston ring profile. The film thickness can be expressed as (Jeng, 1992):

$$h(x,t) = h_m(t) + h_s(x) \tag{2}$$

where h_m is the time varying minimum film thickness and h_s is the ring-face profile. The general ring-face profile can be written as (Jeng, 1992):

$$h_s(x) = \frac{c}{\left(\frac{b}{2}+o\right)^2}(x-o)^2 \tag{3}$$

where c is the crown height, o is the crown offset from the centre of the ring defined to be positive in the x direction, and b is the width of the ring.

2.3 REYNOLDS' BOUNDARY CONDITION

For the first Reynolds's boundary condition, the contact pressure is minimum at point of "rupture" (x_l). Therefore, the first derivative of the contact pressure will become zero at this location. The film thickness at the rupture point will be annotated as h_l, which give the first boundary condition as:

$$\frac{\partial P}{\partial x} = 0 \text{ at } x = x_l \text{ and } h = h_l \tag{4}$$

In order to solve for the integral constant from the integration, a second boundary condition is introduced by assuming the fully flooded inlet condition for the piston ring. Also, the contact pressure at the inlet of the ring is also assumed to be zero. Hence, the second boundary condition can be given as:

$$P = 0 \;\; ; \;\; when\; x = -\frac{b}{2} \tag{5}$$

Thirdly, in order to iteratively solve for the rupture point, $\bar{x}_l$, the contact pressure at the rupture point is assumed to be zero. This leads to the below introduced boundary condition.:

$$P = 0 \;\; ; \;\; when\; \mathrm{x} = x_l \tag{6}$$

2.4 SOLUTION FOR 1-D REYNOLDS' EQUATION

By assuming $U = U_1 + U_2$, the contact pressure is non-dimensionalized using the following terms.

$$tan\bar{x} = \sqrt{\frac{c}{h_o}}\left(\frac{x-o}{\frac{b}{2}+o}\right) \qquad tan\bar{x}_l = \sqrt{\frac{c}{h_o}}\left(\frac{x_l-o}{\frac{b}{2}+o}\right)$$

$$\bar{h}_o = \frac{h_o}{c} \qquad \bar{o} = \frac{o}{c}$$

$$\bar{P} = \frac{h_o^{\frac{3}{2}}\mathrm{P}}{6U\eta_o c^{\frac{1}{2}}} \qquad \bar{b} = \frac{b}{c}$$

which gives the dimensionless pressure as:

$$\bar{P} = \left(\frac{\bar{b}}{2} + \bar{o}\right)\left\{\begin{array}{l} \frac{1}{8}\bar{\bar{x}}_l - \frac{1}{32}sin4\bar{x}_l - tan^2\bar{x}_l\left(\frac{3}{8}\bar{x} + \frac{1}{4}sin2\bar{x}_l + \frac{1}{32}sin4\bar{x}_l\right) \\ \quad -\frac{1}{8}\tan^{-1}\left(-\sqrt{\frac{1}{\bar{h}_0}}\right) + \frac{1}{32}sin4\left(\tan^{-1}\left(-\sqrt{\frac{1}{\bar{h}_0}}\right)\right) \\ \quad +tan^2\bar{x}_l\left\{\begin{array}{l} \frac{3}{8}\tan^{-1}\left(-\sqrt{\frac{1}{\bar{h}_0}}\right) \\ +\frac{1}{4}sin2\left[\tan^{-1}\left(-\sqrt{\frac{1}{\bar{h}_0}}\right)\right] \\ +\frac{1}{32}sin4\left[\tan^{-1}\left(-\sqrt{\frac{1}{\bar{h}_0}}\right)\right] \end{array}\right\} \end{array}\right\} \quad (7)$$

2.5 SOLUTION FOR 1-D ENERGY EQUATION

The temperature of the piston ring and the cylinder liner affects the lubricant temperature. The cylinder liner temperature varies along the top dead centre to the bottom dead centre, which it affects the rate of heat conduction between the piston ring and cylinder liner across the lubricant film. Meanwhile, the relative speed between the piston ring-liner surfaces also varies across the whole engine cycle. This will then affect the shear rate inside the lubricant, making the entrained lubricant to be heated by viscous shearing mechanism. By considering the effect of viscous heating and conduction, the Energy equation is given as follow (Richardson and Borman, 1992):

$$0 = \eta\left(\frac{\partial u}{\partial z}\right)^2 + k\left(\frac{\partial^2 T}{\partial z^2}\right) \quad (8)$$

To obtain an equation for the temperature profile in the oil between the piston ring and cylinder liner, the Energy equation must be solved. With the boundary conditions used in solving the energy equation being the temperature of the cylinder wall and the piston ring face, the temperature profile can now be given as (Richardson et al., 1992):

$$T(z) = -\frac{1}{k}\left[J_2(y)\left(\frac{\partial p}{\partial x}\right)^2 + 2J_2(y)C_a\frac{\partial p}{\partial x} + J_0(y){C_a}^2\right] + (T_r - T_w)\frac{z}{h} + T_w \quad (9)$$

where

$$C_a = \frac{1}{i_0(h)}\left[U - \left(\frac{\partial p}{\partial x}\right)i_1(h)\right]$$

$$i_n(z) = \int_0^z \frac{Z^n}{\eta}d$$

$$I_n(z) = \int_0^z i_n(z)\,dz$$

$$J_n(z) = I_n(z) - I_n(h)\frac{z}{h}$$

2.6 VISCOSITY-TEMPERATURE RELATIONSHIP

The viscosity of the lubricant is dependent on temperature of the lubricant, which in turns affect the load carrying capacity of the lubricant film. The relationship between the viscosity and temperature is governed by the Vogel equation (Harigaya, et al., 2006). It is given as:

$$\eta = a_0 \, e^{\frac{b}{c+T_m}} \tag{10}$$

where a_0, b, c are correlation parameters and T_m is the lubricant mean temperature, which is determined by solving for the Energy equation introduced above.

2.7 SOLUTION FOR FRICTION FORCE

The computed lubricant film profile will be used in predicting the friction force using Greenwood and Williamson model. In this study, the friction force is assumed to consist of two components: a viscous component (f_v) due to lubricant shearing and a boundary component (f_b) due to direct asperity interaction (Chong et al., 2012). For this reason, the friction force for an element area (dA) is given as:

$$df_f = df_b + df_v \tag{11}$$

For an element area, the viscous friction force for a Newtonian fluid can be calculated using the following formula:

$$df_v = \tau(dA - dA_a) \tag{12}$$

where $\tau = \frac{\eta V}{h(x)}$ with V being the sliding velocity, η being the viscosity of the lubricant and dA_a being the asperity contact area. The term τ refers to the shear stress in the lubricant film. Hence, the viscous shear component, τ_v can be computed by dividing the equation (12) by an elemental area (dA). It can be computed as:

$$\tau_v = \frac{\eta V}{h(x)} \frac{(dA - dA_a)}{dA} \tag{13}$$

On the other hand, the boundary friction force results from the shearing of a very thin film with several layers of molecules. It prevails between the interacting asperity tips and exhibits non-Newtonian behaviour. The boundary shear can be predicted using Eyring model (Chong et al., 2012). It can be computed as:

$$df_b = dA_a \left(\tau_o + m \frac{dW_a}{dA_a}\right) \tag{14}$$

Similarly, the boundary shear stress for a single elemental area can be computed by dividing the elemental area (dA). It is computed as:

$$\tau_B = \tau_o \left(\frac{dA_a}{dA}\right) + m \left(\frac{dW_a}{dA}\right) \tag{15}$$

where τ_o is the Erying stress of the lubricant, m is the pressure coefficient of the boundary shear strength and dW_a is the load applied on the asperities for an element's area. In order to determine the asperity contact area, dA_a and the load applied on the

asperities, dW_a, Greenwood and Williamson model can be applied (Chong et al., 2012), which gives:

$$dA_a = dA\pi^2(\zeta\beta\sigma)^2 f_2(\lambda)$$
$$dW_a = \frac{8\sqrt{2}}{15} dA\pi(\zeta\beta\sigma)^2 \sqrt{\frac{\sigma}{\beta}} E^* f_{\frac{5}{2}}(\lambda) \quad (16)$$

where the statistical functions $f_2(\lambda)$ and $f_{5/2}(\lambda)$ are (Teodorescu, et al., 2003):

$$f_2(\lambda) = -0.116\lambda^3 + 0.4682\lambda^2 - 0.7949\lambda + 0.4999$$
$$f_{\frac{5}{2}}(\lambda) = -0.1922\lambda^3 + 0.721\lambda^2 - 1.0649\lambda + 0.6163 \quad (17)$$

with $\lambda = \frac{h(x)}{\sigma}$, $h(x)$ being the film thickness and σ being the combined asperity of piston ring-liner contact surfaces. The composite elastic modulus of the two materials (E^*) from the opposing surfaces can be computed using:

$$\frac{1}{E^*} = \frac{1}{2}\left[\frac{1-{v_1}^2}{E_1} + \frac{1-{v_2}^2}{E_2}\right] \quad (18)$$

where v_1 and v_2 are the Poissons' ratios, E_1 and E_2 are the modulus of elasticity for the material of the piston ring and cylinder liner. Therefore, based on the Greenwood and Williamson friction model, the total friction force along the ring-liner contact can be computed as (Chong et al., 2012):

$$f_{total} = \int_{inlet}^{outlet} (df_v + df_b)\ dx \cdot L \quad (19)$$

3.0 RESULT AND DISCUSSION

The piston ring input parameters of the simulation is shown in Table 1, while the engine parameters and friction model parameter are shown in Table 2 and Table 3, respectively.

Table 1 Piston ring parameters (Jeng, 1992)

Ring Parameters	Values
First Compression Ring	
Ring width, b	1.475 mm
Crown height, c	14.9 µm
Offset, o	0.0 mm
Tangential Tension, T	22.38 N
Second Compression Ring	
Ring width, b	1.470 mm
Crown height, c	5.0 µm
Offset, o	-0.3 mm
Tangential Tension, T	14.05 N
Oil Control Ring	
Ring width, b	0.5 mm
Crown height, c	2.4 µm
Offset, o	0.0 mm
Tangential Tension, T	23.7 N
Distance between upper and lower rail	3.04 mm

Table 2 Engine parameters (Jeng, 1992)

Engine Parameters	Values
Bore diameter, D	0.0889 m
Connecting rod length, l	0.1419 m
Crank radius, R_c	0.04 m
Engine speed, N	2000 rpm

Table 3 Friction model parameters (Teodorescu et al., 2003)

Friction Parameters	Values
σ	0.37 Pa.s
m	0.08
τ_o	2.0 MPa
$\zeta\beta\sigma$	0.055
σ/β	0.001

In the current model, load equilibrium is required for determining the lubricant film thickness in the piston ring-liner contact for a whole engine cycle. The load imposed on the ring is due to two components: 1) the elastic pressure due to the ring's tangential tension 2) the combustion pressure acting at the back of the ring. Therefore, under equilibrium condition, the contact pressure will be equal to the sum of these pressures. The ring elastic pressure can be computed as (Jeng, 1992):

$$p_{elastic} = \frac{2t}{Bb} \tag{20}$$

where t being the tangential tension, B is the cylinder bore diameter and b is the width of the ring.

In this study, the combustion pressure from Jeng's (1992) study is used as an input to the simulation, as it correlates with the same engine parameters used in current simulation. Based on the similar assumption as Jeng (1992), the back of the first compression ring is assumed to expose directly to the combustion pressure, while the second compression ring is only exposed to half of the combustion pressure. It is assumed that the combustion pressure is fully sealed by the second compression ring. Hence, the oil control ring is not exposed to the combustion pressure. The combustion pressure used in the simulation is shown in Figure 1.

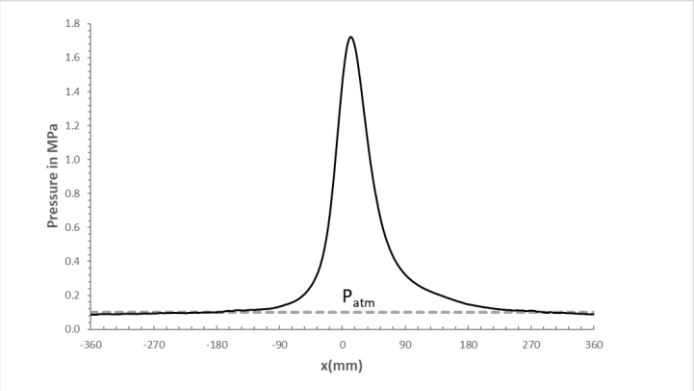

Figure 1 Combustion pressure at 2000 rpm (Jeng, 1992)

Meanwhile, the sliding velocity is assumed to be equal to the velocity of the piston, which the sliding velocity is given as:

$$U = R\Omega\left[\sin\theta + \frac{1}{2}\left(\frac{R}{l}\right)\sin 2\theta\right] \tag{21}$$

The sliding velocity of the piston ring-liner contact at the engine speed of 2000 rpm is shown in Figure 2. For the current study, location A (14°), where the combustion pressure is maximum, is selected to examine the contact pressure, film thickness, temperature profile and friction force along the ring-liner contact.

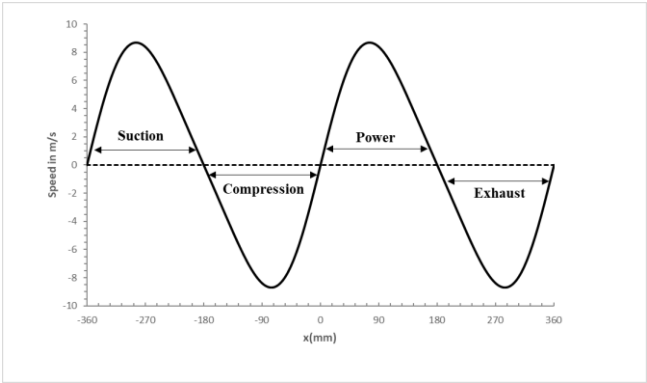

Figure 2 Sliding velocity of piston ring at 2000 rpm

To simulate the temperature profile of the entrained lubricants, the ring temperature is assumed to be constant at 157.7 °C (Harigaya et al., 2006). On top of that, the liner temperature measure by Harigaya et al. (2006) is also taken as an input to the current simulation.

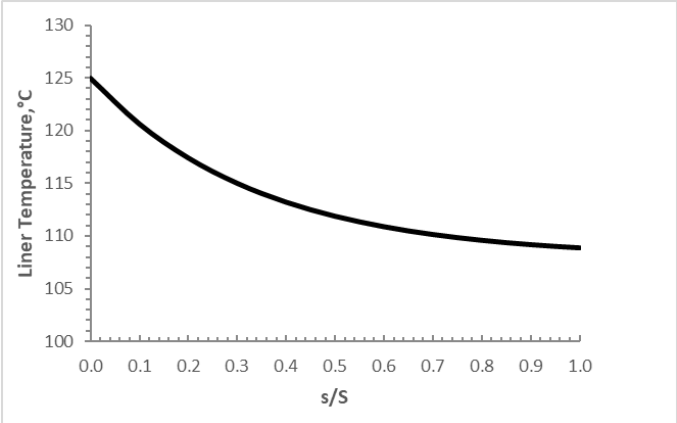

Figure 3 Measured cylinder liner temperature (Harigaya et al., 2006)

In this study, the lubricant grade that was used in the simulation is SAE 5W30. The viscosity of the lubrication at a particular mean temperature is estimated using the Vogel equation, which is given as (Deligant et al., 2011):

$$\eta(T_m) = 7.48 \times 10^{-5}\, e^{\frac{1005.2}{115.7+T_m}} \tag{22}$$

where η is the viscosity in Pa.s and T_m is the mean temperature in °C.

3.1 CONTACT PRESSURE DISTRIBUTION

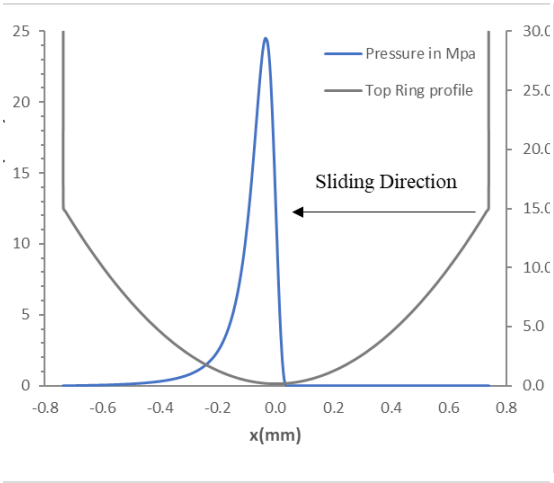

A.) Top Compression Ring

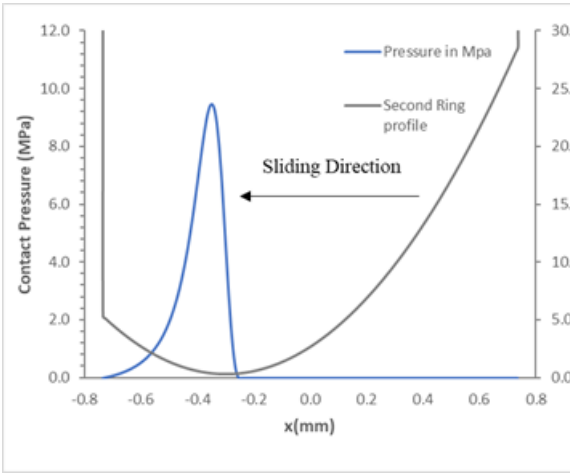

B.) Second Compression Ring

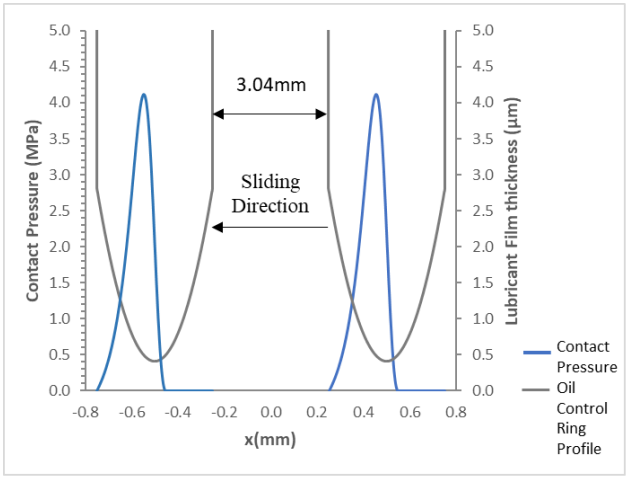

C.) Oil Control Ring

Figure 4 Contact pressure of the entrained lubricant for the ring pack at crank angle 14°.

Based on Figure 4, among all three piston rings, the highest contact pressure was found in the first compression ring. This corresponds to the higher combustion pressure acting at the back of the top compression ring, resulting in a peak contact pressure around 25 MPa. The peak contact pressure in the second compression ring is around 9.5MPa, where the contact pressure distribution is spread over a narrower region due to the smaller convex shape at the lubricant flow inlet, limiting the lubricant entrainment in the contact.

The contact pressure decreases from top compression ring to the oil control ring, which it mainly due to the assumption that the combustion pressure is completely sealed off by the second combustion ring, resulting in no load imposing on the oil control ring except the tangential tension of the ring. The oil control ring, which consists of two identical and symmetrical narrow rings, namely upper and lower rail. In the current study, these rails are separated by a fixed distance of 3.04mm, which is given by Jeng (1992).

3.2 Lubricant temperature Profile Distribution

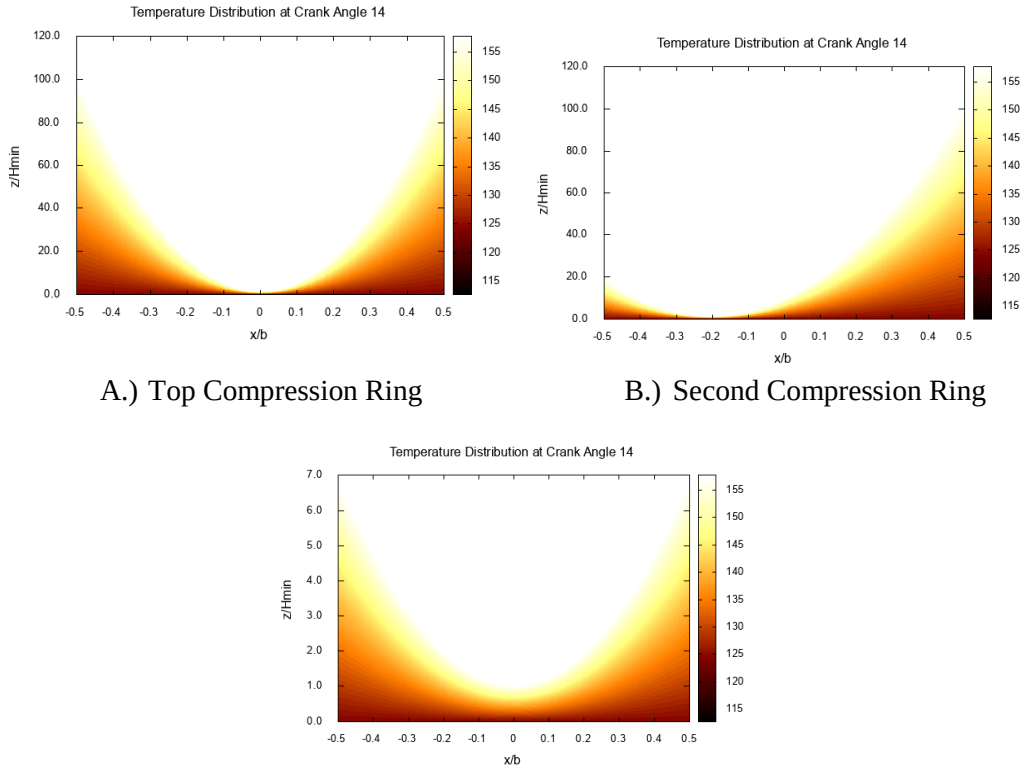

A.) Top Compression Ring B.) Second Compression Ring

C.) Oil Control Ring

Figure 5 Temperature profile of the entrained lubricant for the ring pack at crank angle 14°

The temperature profile of the entrained lubricant is computed using the 1D energy equation solutions. Overall, it was observed that the effect of heat conduction is far more predominant than the viscous heating effect at engine operating condition, where a linear change in temperature is observed across the ring-liner boundary for all three piston rings. The heating effect of lubricant due to viscous shearing is not significant. This is because the width of the ring contact is small, causing the entrained lubricant to unable to generate significant amount of heating effect from viscous shearing mechanism. Figure 5 (C) shows the temperature profile of one of the rail in the oil control ring, where the other rail is assumed to have the same temperature profile.

3.3 MINIMUM FILM THICKNESS

Based on the same computational procedures, the lubricant film thickness can be computed for each individual piston ring along the whole engine cycle. The calculation of film thickness is vital for examining the friction in the ring-liner contact. This is because the lubricant film profile will be used as an input to calculate the shear stress and friction in the ring-liner contact along the whole engine cycle. From Figure 6, the peak of minimum film thickness is lowest along the power stroke. This is due to the higher load imposed on the top compression ring and second compression ring during the power stroke.

For the second compression ring, during the compression and exhaust stroke, the second compression ring moves upward and the ring slide to the right computational domain and vice versa for the suction and power stroke. Based on Figure 6, the minimum film thickness is significantly lower along the suction and power stroke, which is when

the second compression ring slides downwards. It is observed that the lubricant film will be thinner when the lubricant flow from a smaller convex area. Again, the thinnest film is occurred along the ignition stroke, since half of the combustion pressure is still imposing load to the second compression ring. Overall, the minimum film thickness is thicker for the second compression ring along the whole engine cycle as compared to the top compression ring. This is mainly due to the reducing load imposed on the second compression ring.

Meanwhile, even though that the load imposed on the oil control rings are lower due to the absence of compression pressure, the minimum film thickness of the oil control ring is lowest among the three rings. However, this can be explained by the main function of the oil control ring, which scrapes the remaining lubricant along the cylinder liner.

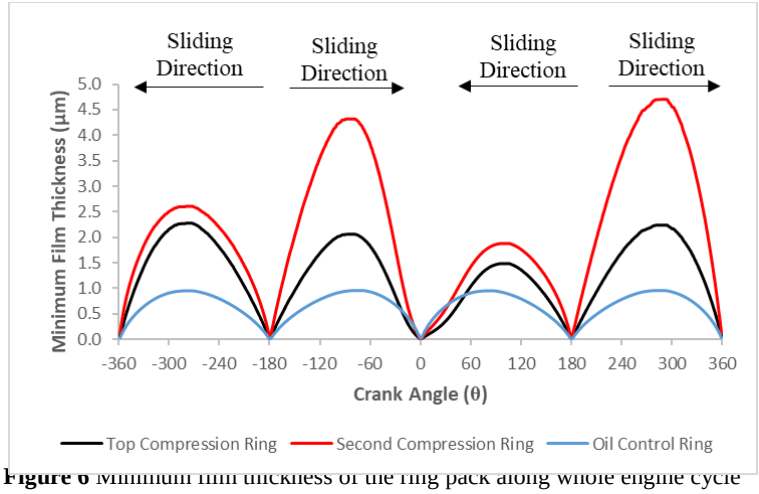

Figure 6 Minimum film thickness of the ring pack along whole engine cycle

3.4 TOTAL FRICTION FORCE

After summing up the viscous and boundary friction, the total friction force over the complete engine cycle is computed as shown in Figure 7. Overall, the boundary friction force predominates the contribution of viscous friction, especially at the point of reversals. The highest total friction force is again being observed to locate along the vicinity of power stroke. This can be explained by the high load being imposed on the ring that cycle region.

Figur

Similarly, the total friction generated by the second compression ring along the whole engine cycle is shown in Figure 8. The highest total friction recorded for the second

compression ring is 94.2 N at the vicinity of dead centre. Overall, the friction generated from the second compression ring is less than the top compression ring. This is due to the fact that smaller load is imposed on the second compression ring as compared to the top compression ring, where smaller compression pressure acting on the second compression ring due to engine blow-by.

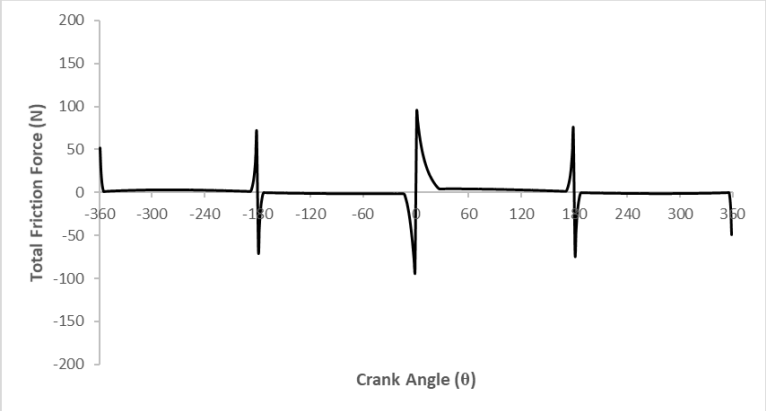

Figure 8 Total friction force of second compression ring along whole engine cycle at 2000rpm

Lastly, the total friction force of the oil control ring is depicted in Figure 9. A symmetrical pattern of total friction was shown along the whole engine cycle This is because a constant load is being imposed on the oil control ring and the variation is only at the change of sliding velocity, which it varies in symmetrical pattern. The total friction generated by the oil control ring is the highest among the piston rings. This is because the oil control ring is made up of two identical rails, which the total friction is the sum of the two rails.

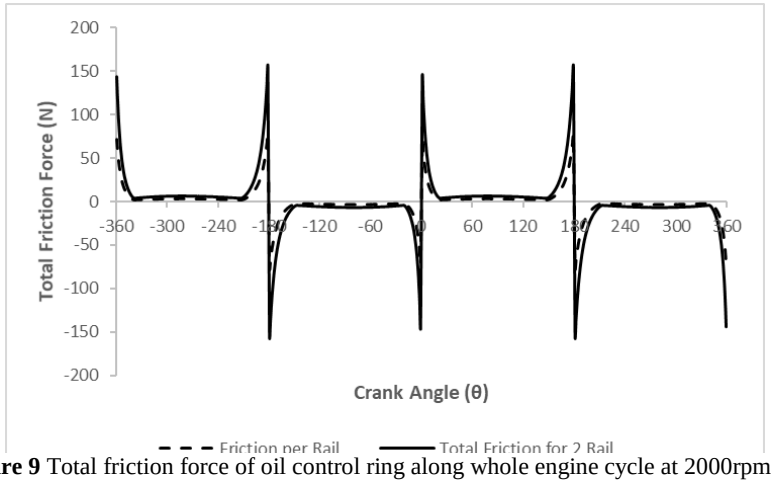

Figure 9 Total friction force of oil control ring along whole engine cycle at 2000rpm

3.4 TOTAL FRICTIONAL FORCE OF PISTON RINGS PACK ALONG THE RING-LINER CONJUNCTION

The total friction force generated by the ring pack can be determined by summing all the total friction force of individual piston rings. The total friction force for the piston ring pack along the whole engine cycle is shown in Figure 10. The largest friction force is 337.8N over a complete engine cycle at 2000rpm, which it happened at the vicinity of piston motion reversal from compression stroke to power stroke at top dead centre.

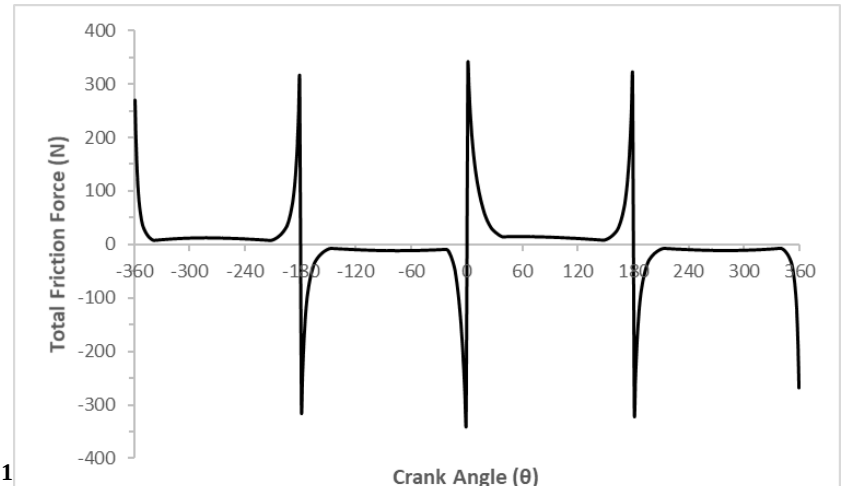

Figure 1

3.4 SIMULATION MODEL VALIDATION

In order to validate the current simulation model with the isothermal simulation model proposed by Jeng (1992), the model has changed by using a fixed value of viscosity (0.0689 Pa.s). The minimum film thickness across whole engine cycle is shown in Figure 11. It is observed that the simulated lubricant film thickness follows the same trends as the literature data. However, Jeng (1992) run its simulation by setting the lowest minimum film thickness to be equal to the surface roughness (0.37μm). He modelled the boundary friction in this region using the Coulomb friction (F=μN), which is a different from the Greenwood and Williamson friction model used in current study.

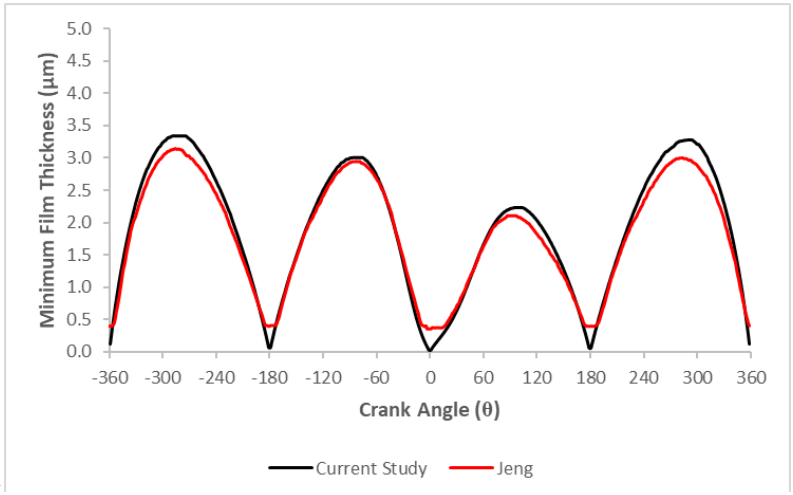

Figure 11 data

The total friction force generated by the top compression ring along the whole engine cycle is shown in Figure 12. It was observed that the simulated total friction force using the Greenwood and Williamson model is shown to be higher than Jeng's (1992) study, especially during the vicinity of piston motion reversals at dead centres. This is believed to be the result of the method used by Jeng (1992) in limiting the minimum film thickness, causing his model to estimate a thicker film and lower boundary friction force in the dead centres. However, the computed total friction using current model correlates well with the trend in the literature data. The highest total friction force in both study also shown to occur along the vicinity of power stroke, which is due to higher load being imposed on the ring during the high combustion pressure generated from ignition.

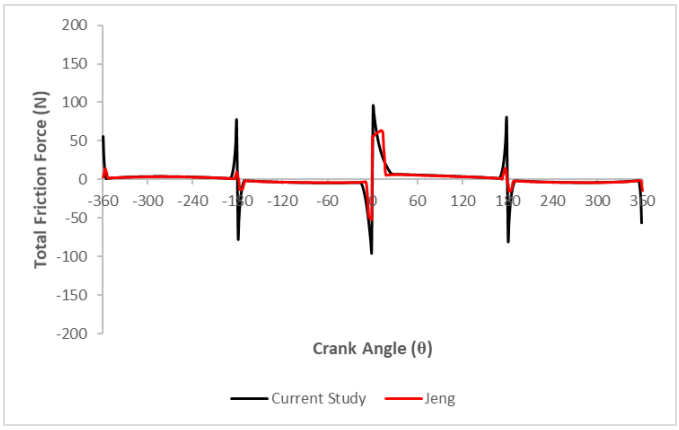

Figure 12 Validation of total friction force of the top compression ring with literature data

3.6 ALTERNATIVE METHODS TO ESTIMATE LUBRICANT TEMPERATURE

The method shown in the current study involves the usage of 1D energy equation to model the heat transfer across the lubricant in the ring-liner boundary, which is considered to be more computational expensive over the isothermal counterpart. Aside from using 1D energy solution as the current study, there are several methods that may be used to estimate the viscosity of the entrained lubricants. The simplest method will be using an isothermal assumption and assume that the viscosity is constant across the whole engine cycle. Besides these, the lubricant temperature can be assumed to be the same as the cylinder liner (Richardson and Borman,1992). Both the methods are adapted to the 1D Reynolds' solution to compare the changes in computing the minimum film thickness. The result of comparing the methods for the top compression ring is shown in Figure 13.

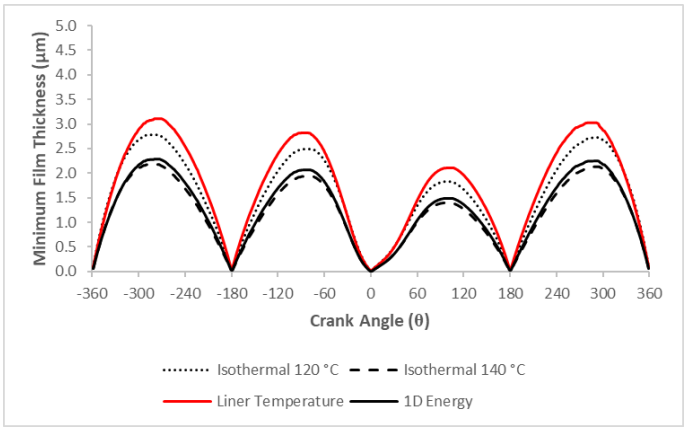

Figure 13 Computation of minimum film thickness for the top compression ring using different methods to estimate lubricant temperature

It was observed that if the lubricant's viscosity is estimated using the liner temperature, the minimum film thickness will be the largest across the whole engine cycle. While on the other hand, the minimum film thickness when the assumed constant lubricant temperature of 140 °C will be lower than the 120°C counterparts. This is due to the decrease of load carry capacity of the lubricant when the viscosity of the lubricant is decreased at higher temperature. Based on the current study, using the assumption of 140 °C for the lubricant temperature will give a closer estimation of minimum film thickness as the solution of computing using 1D energy equation. Although solving the lubricant film formation with the isothermal assumption will help to simplify the solution and save a lot of computational time, the selection of input temperature for the lubricant to model the lubricant film thickness remains a challenge.

Using different methods to estimate the viscosity of the lubricant in the ring-liner conjunction could have a significant impact towards the viscous friction force of the top compression ring. The viscous friction force and boundary friction force generated by the top compression ring using all three methods are shown in Figure 14 and Figure 15. Generally, it was observed that using the viscosity computed from the liner temperature for solving the viscous friction will give the highest viscous friction along the whole engine cycle. On the other hand, using an isothermal assumption with lubricant at 140 °C gives the lowest viscous friction among other methods. This is because viscous shearing is less significant at elevated temperature, smaller viscous friction is generated as the viscosity is decreased. In contrast, the boundary friction computed using all three methods do not show any significant changes. This is because the boundary friction computation is independent to the viscosity of the lubricant.

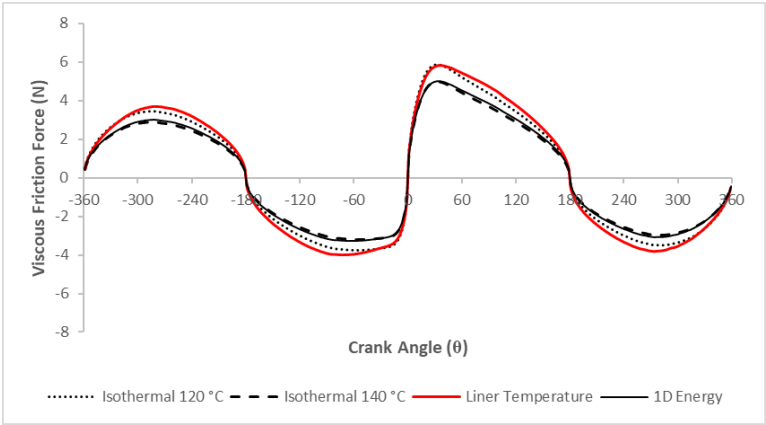

Figure 14 Computation of viscous friction force for the top compression ring using different methods to estimate lubricant temperature

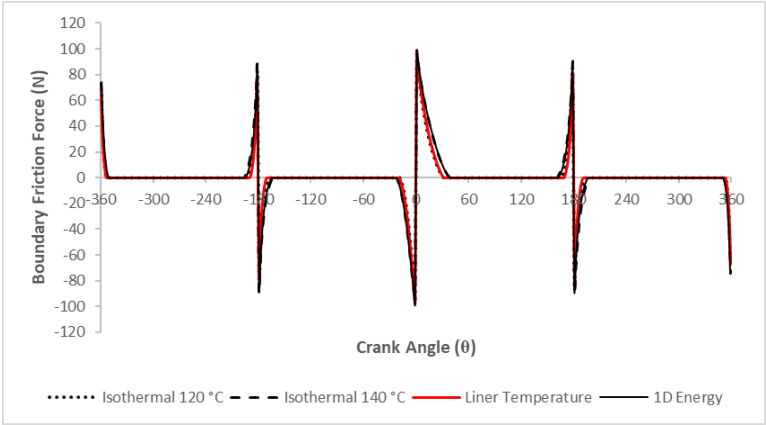

Figure 15 Computation of boundary friction force for the top compression ring using different methods to estimate lubricant temperature

4.0 CONCLUSION

The results of minimum film thickness and total friction force for the current model is validated and compared with the literature data. The mathematical model of the current study correlates well with the published data, which the same trends of total friction force is observed across the whole engine cycle. The total friction force peaks along the vicinity of piston motion reversal, with the maximum friction force observed at the top dead centre during the transition from compression stroke to power stroke. This attributes to the load imposed by the combustion pressure on the top and second compression ring due to engine blow-by.

Overall, the temperature distribution across the ring-liner boundary is shown to vary in a linear pattern. This signifies the heat conduction heat transfer predominate the viscous heating effects, where temperature rise due to viscous shearing is hardly noticeable due to the small contact area along the ring-liner conjunction. If the system is assumed to be isothermal and the lubricant viscosity is assumed to be constant based on the assumed temperature, the viscous frictional force simulated can be very close to the result computed from 1D energy equation. Assuming the system to be isothermal may reduce the computational time. However, selection of the assumed lubricant temperature for thermal analysis remains a challenge. But overall, the total friction force generated by the piston ring sliding along the engine cylinder for a whole engine cycle does not show a significant difference when the alternative approaches were used.

In short, heat transfer affects the viscous friction force in the piston ring-liner contact for a whole engine cycle. Overall, boundary friction predominates the contribution of viscous friction, especially along the vicinity of dead centres. However, the boundary friction is not affected by the changes in lubricant viscosity. Hence, the effect of heat transfer towards total friction force generated by the ring pack along a whole engine cycle could be considered trivial.

ACKNOWLEDGEMENT

The author acknowledges the support and guidance from supervisor, Dr. William Chong Woei Fong and appreciates Universiti Teknologi Malaysia (UTM) for providing facilities and literature resources.

REFERENCES

[1] Chong, W.W.F. (2012). Adhesive and molecular friction in tribological conjunctions. PhD Thesis, Cranfield University, England.

[2] Deligant, M., Podevin, P., & Descombes, G. (2011). CFD model for turbocharger journal bearing performances. *Applied Thermal Engineering*, *31(5)*, 811-819.

[3] Hamrock B.J., Schmid S.R., Jacobson B.O. (2004). *Fundamentals of fluid film lubrication*, CRC press.

[4] Harigaya, Y., Suzuki, M., Toda, F., & Takiguchi, M. (2006). Analysis of oil film thickness and heat transfer on a piston ring of a diesel engine: effect of lubricant viscosity. *Journal of engineering for gas turbines and power*, *128*(3), 685-693.

[5] Holmberg, K., Andersson, P., & Erdemir, A. (2012). Global energy consumption due to friction in passenger cars. *Tribology International*, *47*, 221-234.

[6] Jeng, Y. R. (1992). Theoretical analysis of piston-ring lubrication Part I—fully flooded lubrication. *Tribology Transactions*, *35*(4), 696-706..

[7] Rahmani, R., Rahnejat, H., Fitzsimons, B., & Dowson, D. (2017). The effect of cylinder liner operating temperature on frictional loss and engine emissions in piston ring conjunction. *Applied energy*, *191*, 568-581.

[8] Richardson, D.E., & Borman, G.L. (1992). Theoretical and experimental investigations of oil films for application to piston ring lubrication. *SAE Technical Paper*.

[9] Teodorescu, M., Taraza, D., Henein, N. A., & Bryzik, W. (2003). Simplified elasto-hydrodynamic friction model of the cam-tappet contact. *SAE transactions*, 1271-1282.